Journal of Energetic Materials
Publication details, including instructions for authors and subscription information:
http://www.informaworld.com/smpp/title~content=t713770432

Characterization of Fe/$KClO_4$ Heat Powders and Pellets

Ronald A. Guidotti[a]; Judy Odinek[a]; Frederick W. Reinhardt[a]
[a] Sandia National Laboratories, Albuquerque, NM

To cite this Article Guidotti, Ronald A. , Odinek, Judy and Reinhardt, Frederick W.(2006) 'Characterization of Fe/$KClO_4$ Heat Powders and Pellets', Journal of Energetic Materials, 24: 4, 271 — 305
To link to this Article: DOI: 10.1080/07370650600896566
URL: http://dx.doi.org/10.1080/07370650600896566

Journal of Energetic Materials, 24: 271–305, 2006

ISSN: 0737-0652 print/1545-8822 online
DOI: 10.1080/07370650600896566

Characterization of $Fe/KClO_4$ Heat Powders and Pellets

RONALD A. GUIDOTTI
JUDY ODINEK
FREDERICK W. REINHARDT

Sandia National Laboratories, Albuquerque, NM

Pellets of $Fe/KClO_4$ mixtures are used as a heat source for thermally activated (''thermal'') batteries. They provide the energy necessary for melting the electrolyte and bringing the battery stack to operating temperature. The effects of morphology of the Fe and the heat-pellet density and composition on both the physical properties (flowability, pelletization, and pellet strength) and the pyrotechnic performance (burn rate and ignition sensitivity) were examined using several commercial sources of Fe.

Keywords: burn rate, $Fe/KClO_4$, heat powders, ignition sensitivity, thermal batteries

Introduction

Thermally activated (''thermal'') batteries designed by Sandia National Laboratories (SNL) for the Department of Energy are designed to have a shelf life of 25 years or more. These batteries depend on a molten salt as the medium for ionic transport during discharge. Until the electrolyte becomes molten, the batteries are totally inert, which is responsible for the long storage life. To melt the electrolyte, each cell in the stack requires

Address correspondence to Ronald A. Guidotti, Sierra Nevada Consulting, 1536 W. High Pointe Ct., Minden, NV 89423. E-mail: RonGuidotti@SierraNevadaConsulting.com

a pyrotechnic heat source to bring the cell to the desired operating temperature, typically between 450 and 550°C. The initial heat source for such batteries was a heat paper based on $Zr/BaCrO_4$ blended with ceramic fibers. This material, however, suffered from several major problems. It was not electrically conductive after combustion, which required the use of additional hardware to electrically connect cells in a battery stack in series. In addition, it was very static and shock sensitive, which made it hazardous to handle in large quantities.

In the late 1960s, an extensive research effort was undertaken by SNL at Unidynamics/Phoenix to find a more suitable alternative to heat paper [1]. This work was documented by Guidotti [2]. As all of the active stack components in a thermal battery are pelletized from powder mixtures, the use of a pelletized heat source was desired. A number of characteristics were used for screening purposes. These included:

- Physical strength of the heat pellets and ease of pelletization
- Calorific output
- Gas evolution
- Ignitability by 360 cal/g $Zr/BaCrO_4$ heat paper (used as a fuze)
- Relative ignition sensitivity
- Linear burn rate
- Electrical conductivity
- Combustion temperature
- Dimensional stability

A wide range of combinations of fuels and oxidizing agents was explored and the one combination that stood out above all others was one based on Fe and $KClO_4$. The composition of the heat powders used in thermal batteries is such that all mixtures are fuel rich (i.e., oxidant limited), so that a porous Fe disc results after combustion. This then provides a means of electrically connecting cells together in a battery stack. The $Fe/KClO_4$ system has a high calorific output, about 710.9 cal/g of mixture at the stoichiometric composition of

61.8% Fe/38.2% $KClO_4$, as illustrated in Eq. (1).

$$4Fe + KClO_4 \longrightarrow 4FeO + KCl \tag{1}$$

This reaction has been verified by x-ray diffraction analysis of burned pellets. Mixtures of Fe and $KClO_4$ are easy to pelletize and form strong pellets. They are almost gasless and maintain good dimensional stability after combustion. Pellets of these materials also have fairly high burn rates.

Although there has been some effort in the past to characterize the physical properties of Fe/$KClO_4$ blends, the effort has not been totally comprehensive or systematic. McCarthy et al. studied the effect of pellet density on the burn rate [3]. However, only two compositions were examined in that work. Evans examined the ignition sensitivity of such materials using a capacitive-discharge (CD) approach, but, again, only over a limited range of experimental conditions [4]. Guidotti et al. reported on the burn characteristics of Fe/$KClO_4$ heat pellets over a range of compositions, from 80% Fe to 88% Fe [5]. The effects of pellet density on the burn rate and ignition sensitivity were also examined. Callaway et al. reported on similar work involving several sources of Fe, including carbonyl Fe [6]. In this work, we have extended our original work to include a number of sources of carbonyl Fe. This form of Fe is of interest because heat powders with this Fe exhibit lower burn rates than the conventional counterparts. In addition, they may have higher bulk densities. There are times when lower burn rates are desired for heat pellets in thermal batteries but that are not readily attainable with the current heat powders, where there is little or no control over the Fe particle size.

In addition to the thermal properties of such pyrotechnic materials, there are a number of critical physical (mechanical) properties that are just as important for proper pelletization. A pyrotechnic blend that cannot be readily pressed into strong pellets or that has poor handling properties is of little use as a thermal-battery heat source. Consequently, we have developed a number of metrics that allow relative pelletization parameters to be determined.

Experimental Procedures

Materials

The Fe/$KClO_4$ heat powders were obtained from three sources: EaglePicher Technologies (EPT, Joplin, MO), Unidynamics/Phoenix, Inc. (UPI [now Pacific Scientific, Inc.], Chandler, AZ), and Pyrotechnic Specialties, Inc. (PSI, Byron, GA). Compositions of the blends studied were (in Fe/$KClO_4$ weight ratios): 88/12, 86/14, 84/16, 83/17, 82/18, 81/19, and 80/20. Not all compositions were tested for each manufacturer. The 80/20 blend was made in house by addition of $KClO_4$ to an existing 84/16 composition. After blending, the resulting mixture was passed through a 100-mesh sieve to eliminate any agglomerates. The $KClO_4$ used in all mixes was from Barium & Chemicals (Steubenville, OH), made to the Mil-P-217A specification.

The source of Fe used for the UPI heat powders is NX-1000 (Ametek, Eighty Four, PA), but the sources of Fe for the EPT and PSI materials are not known. In addition to these standard Fe powders, several sources of spheroidal carbonyl Fe from BASF (81941 and 81931) and ISP (S-1000, S-2101, and S-3700) were examined along with acicular Fe from Domfer (MP31 and MP64) in an 84/16 composition made in-house. Fe from OMG (Cleveland, OH) was also examined.

Processing

Pellets used in the study were 1.25″ (38 mm) in diameter and weighed $\sim$3.8 g. The thickness was varied to obtain the desired pellet densities of 55–85% theoretical density (TD) (45–15% porosity). Materials were processed, pelletized, and stored in a dry room where the relative humidity was maintained at $<$3%. The burn rate and ignition sensitivity measurements were also conducted in the same dry room.

Chemical Analysis

The oxygen level in the Fe used in the various heat powders was measured using inert-gas fusion (IGF). In earlier work by Guidotti, it was demonstrated that this provided equivalent

results to fast-neutron (14 MeV) activation [2]. The IGF technique was much quicker and less expensive.

Break Strength

The break-strength test setup was based on a 10-pound Ametek force gauge coupled with a Chantillon readout. The test pellet was placed on two resting supports and then the ram with a knife edge attached was driven downward at a constant speed until it pressed against the pellet, breaking it. The maximum force that registered on the digital display was recorded for each test. Three samples were tested for each set of conditions (e.g., composition and % TD). There was an inverse relationship between the ram speed and the observed pellet break strength. A speed of 2 in/min was used for all of the break-strength tests in this study. Typically, the standard deviation around the mean break strength was less than 2%.

Particle Size Analysis

The specification for SNL's heat powder calls out an average Fe particle size of 1.5–3.5 μm as determined by the Fisher subsieve sizer. This technique measures the pressure drop across a packed bed of powder and assumes spherical particles. It is not a very good method for particle-size measurement as it provides no data as to the distribution of particle sizes and assumes a spheroidal particle morphology. The Sedigraph 5000 or the Leeds-Northrop Microtrak both depend on the sedimentation technique and provide a good measure of particle-size distribution. However, data from one machine cannot be directly compared to data from the other. The Sedigraph 5000 uses an x-ray beam for particle-size characterization, while the Microtrak uses visible light for this same purpose. For example, one lot of heat powder had an average Fe particle size of 10 μm as determined by the Sedigraph 5000. When tested with the Microtrak, this same material showed a much higher average particle size of 14.6 μm.

The Sedigraph 5000 was used for measurement of the particle size of the Fe and, in a limited number of tests, that for

$KClO_4$. Sedisperse A-13 was used as the medium for Fe particle-size measurements. The Fe powder was mixed with the Sedisperse A-13 and then ultrasonically agitated for 10 min prior to a run. (Because of the magnetic nature of the Fe, a magnetic stirrer could not be used to maintain the materials in suspension.) To obtain the Fe samples from pre-made heat powders, the heat powders were leached in deoxygenated water for 5 min to remove $KClO_4$. The slurry was then quickly filtered and washed with acetone and vacuum dried at room temperature. In the case of tests with $KClO_4$, the samples were stirred in Sedisperse P-11 using a magnetic stir bar to collect the Fe. The $KClO_4$ slurry was then decanted from the beaker and the medium removed by filtration. The $KClO_4$ was then washed with toluene and ethanol and vacuum dried as for the Fe.

Calorific Output

Samples of the various heat powders were analyzed for calorific output in a Parr adiabatic bomb calorimeter under an argon atmosphere. Sample sizes of 4–5 g gave good results. These measurements were made in triplicate.

Burn Rate

It was not feasible to measure both the ignition sensitivity and the burn rate with the same experimental setup. Instead, a separate test fixture, shown schematically in Fig. 1, was devised for the burn rate measurements. The setup was designed to also record the peak temperature of the pellet during burning.

The heat pellet was held between two 3-mm-thick squares of Min-K® TE1400 to insulate it. A piece of mica was inserted between the Min-K® pads and the heat pellet to protect the Min-K® and the quartz rods that served as light guides for the photodiode fiber optic cable inserted in the top aluminum plate. The photodiodes had incorporated into them a fiber optic cable, which greatly facilitated construction and design of the test fixture.

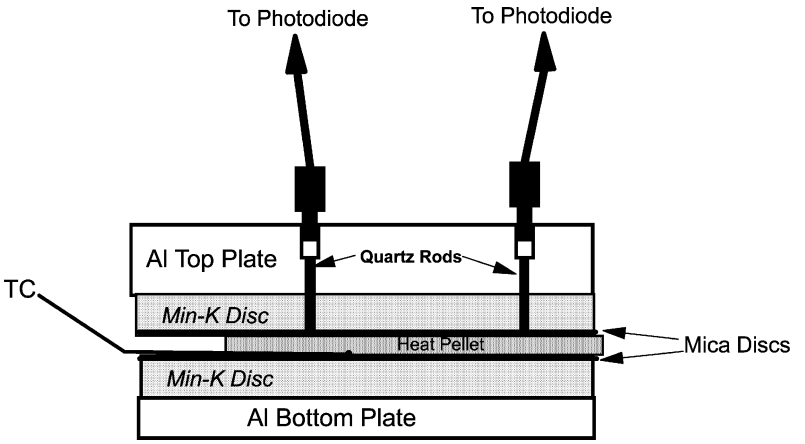

Figure 1. Schematic diagram of test fixture for measurement of burn rate and peak temperature of Fe/$KClO_4$ heat pellets.

Either a flattened, 32-gauge (0.315-mm dia.) type-K (Chromel-Alumel®) or type-R (Pt/10% Pt-Rh) thermocouple (rated to 1,700°C) was inserted between the mica and bottom Min-K® pad to measure the temperature during burning. An electronic interface provided a TTL signal output to a counter when the photodiode was triggered by the light emitted from the burning heat pellet. The second photodiode was triggered when the burn front reached it, providing the necessary timing for burn rate calculations over the fixed, known distance (12.7 mm). A propane torch was used to initiate the burning of the heat pellet by application to the exposed tip of the heat pellet extending from the test fixture.

Ignition Sensitivity Measurements

The ignition sensitivity was determined using a custom 20-W solid-state diode laser, whose output was controlled by a constant-current power supply. The laser and power supply were designed and built by Quantic Industries, Inc. (Hollister, CA). The laser energy was controlled by the amplitude and width of the output pulse, which could be varied from 100 to

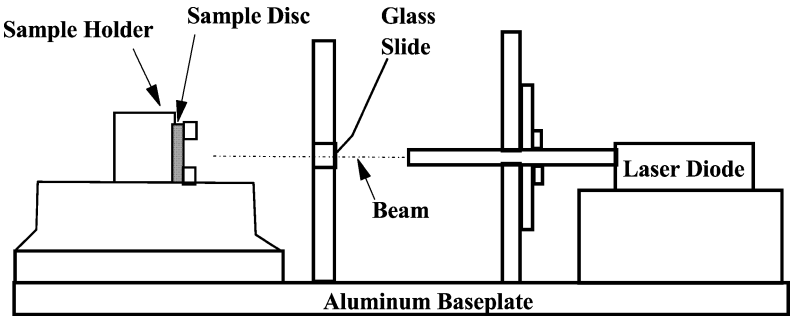

Figure 2. Schematic of laser and sample setup for ignition-sensitivity measurements.

400 ms. A Scientech Model S310 energy meter was used to calibrate the laser diode output with the corresponding current setting of the power supply and to periodically measure the energy during testing. A welded aluminum box was designed to hold the laser, energy meter, and sample holder. The stability of the laser was excellent so that it was not necessary to measure the energy after each firing. This greatly extended the lifetime of the diode laser. There was no measurable drift after over 100 firings of the laser. A schematic of the laser and sample setup used for ignition sensitivity tests is shown in Fig. 2.

A modified Bruceton method was used for ignition sensitivity determinations, with an energy increment of 0.05 J for the tests [7]. Up to six shots were allowed per pellet (after rotation of 45° between shots) before the pellet was discarded. Up to 20 pellets were used to define the data set for a given set of conditions (e.g., composition and density).

Results and Discussion

Physical Properties

Morphology. The morphology of the Fe powders can have a major impact on the physical properties of heat powders in which they are used. A typical scanning electron microscopy (SEM) photomicrograph of the standard Ametek NX-1000 Fe

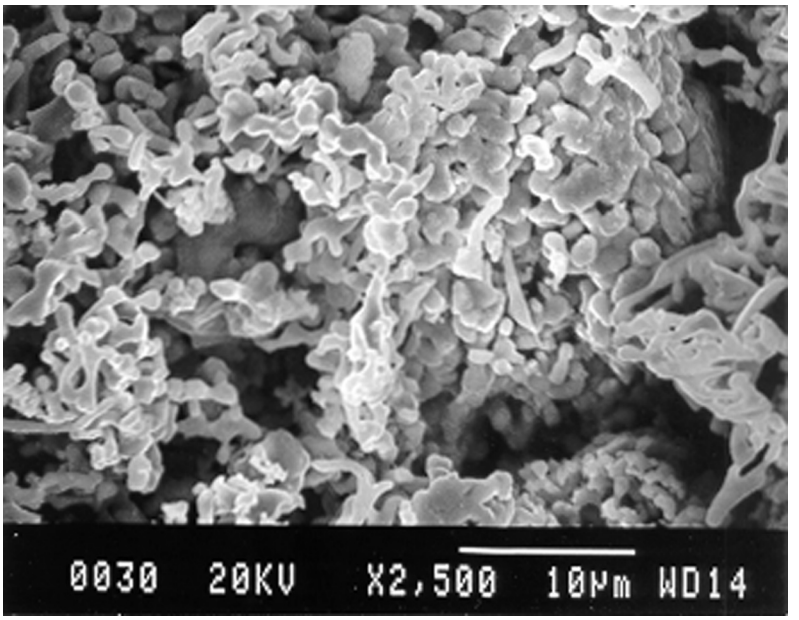

Figure 3. SEM photomicrograph of NX-1000 Fe powder (10 µm marker).

powder used in the UPI heat powders is shown in Fig. 3. This material has an elongated, interlocking structure. Similar features are evident for the Fe used in the EPT and PSI heat powders (Figs. 4 and 5, respectively) and for the OMG Fe (Fig. 6). This morphology contrasts with that of the carbonyl Fe materials. The morphology of the Domfer Fe is rather chunky and acicular (Fig. 7), while that of the ISP and BASF Fe powders is very spheroidal (Figs. 8 and 9, respectively). Heat powders made with the spheroidal Fe materials might be expected to flow into die cavities more easily and pack more readily (i.e., have a higher bulk density) but might produce pellets that lack the strength of those made with elongated Fe particles, such as NX-1000.

The angle of repose gives a measure of flowability of powders, with a more free-flowing material exhibiting a lower angle. The bulk density provides information on the packing of a

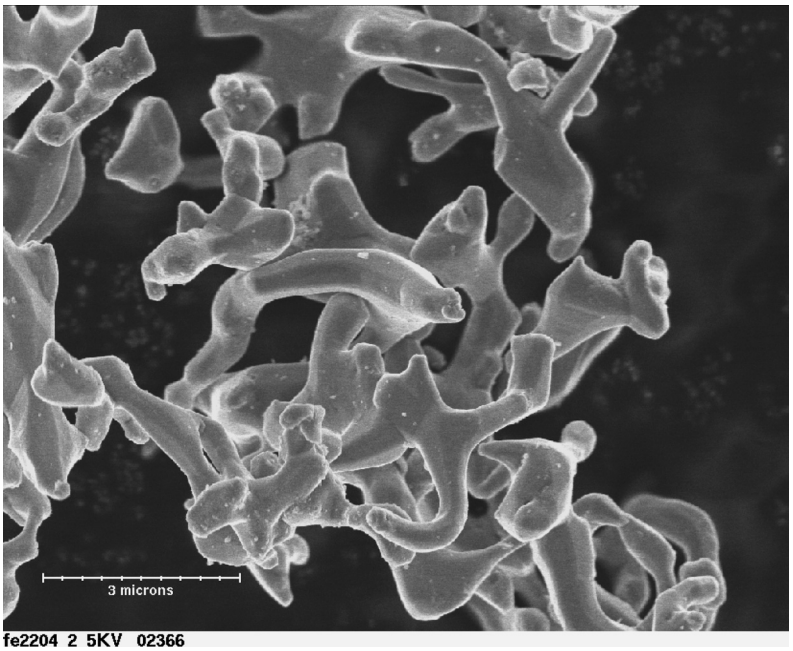

Figure 4. SEM photomicrograph of Fe powder used in EPT heat powder (3 μm marker).

powder. A higher bulk density means more material can be placed in the fixed volume of a die cavity during pelletizing. Data for these two properties are summarized in Table 1 for an 86/14 composition along with the average particle size as determined by the Sedigraph 5000.

The angle of repose for heat powders made with the ISP Fe ranged from 58.5 to 66.5°, with bulk densities of 2.25–3.18 g/cc. Similar angle-of-repose data for the heat powders made with BASF Fe were 46.6–52.2° with bulk densities of ∼3.11 g/cc. This compares to angles of repose of 50.0–54.0° and bulk densities of 3.34–3.48 g/cc for heat powders made with the Domfer Fe, which had the highest bulk densities with intermediate angles of repose. The standard heat powder made with NX-1000 Fe had the lowest bulk density and an angle of repose similar to those for the heat powders made with Domfer Fe.

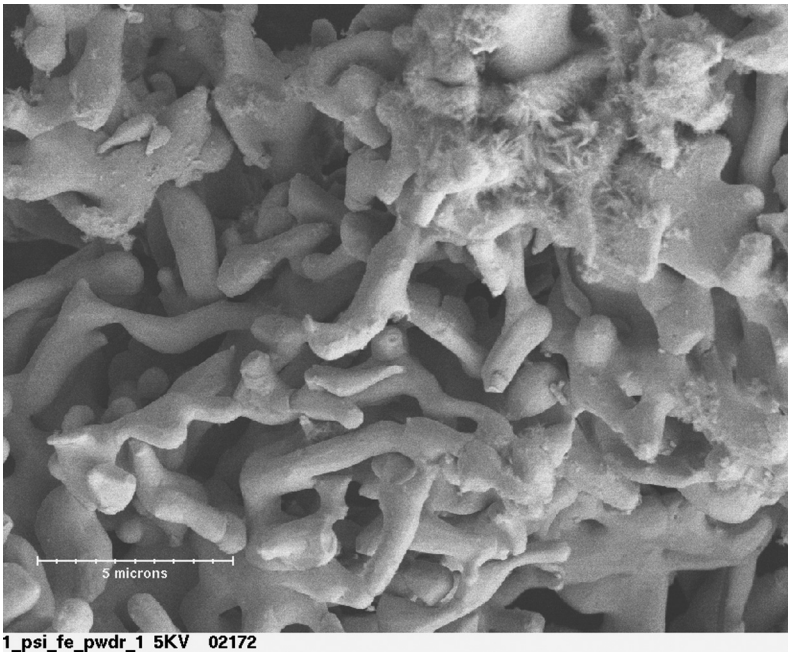

Figure 5. SEM photomicrograph of Fe powder used in PSI heat powder (5 μm marker).

The heat powders made with the spheroidal BASF Fe had good flow properties and spread in the die easily but could not be readily consolidated. Heat powders made with the spheroidal ISP Fe also spread relatively easily in the dies but still could not be consolidated. Heat powders made with the acicular Domfer Fe were better in both cases and these materials had the largest particle size and highest bulk density. This is consistent with results reported by Callaway et al. [6]. However, pellet integrity was deficient relative to heat pellets made with the conventional Fe powders.

Forming Pressure. The forming pressure was recorded for the various densities and compositions as complementary physical data for the Fe/$KClO_4$ heat pellets. The logarithm of the forming pressure is plotted vs. % TD for the 88/12

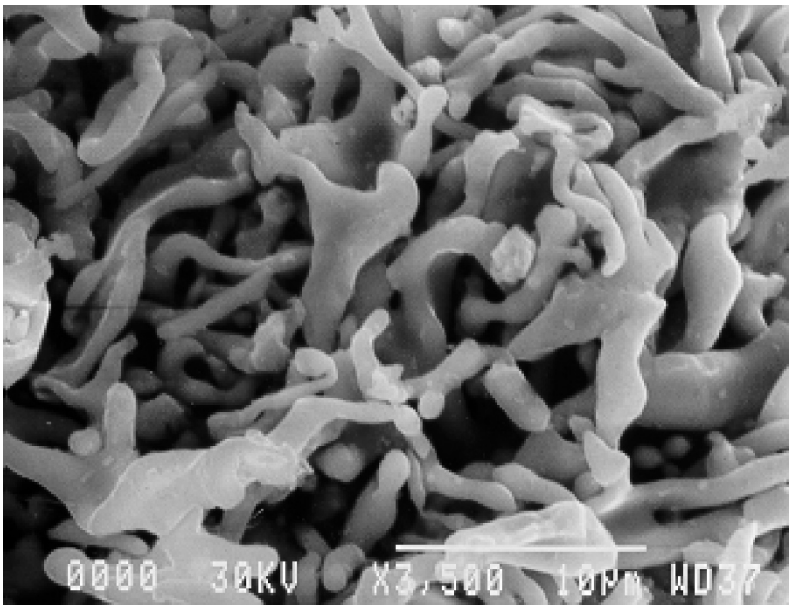

Figure 6. SEM photomicrograph of OMG Fe powder (10 µm marker).

composition for the NX-1000 Fe in Fig. 10 and shows a linear relationship. Similar behavior but with different slopes was also observed at other compositions and with other sources of Fe. Forming-pressure data are summarized in Table 2 for various compositions for a number of Fe sources along with the measured average particle sizes. (The average particle size of the $KClO_4$ was 12.8 µm.) Data were not available for heat powders made with the carbonyl Fe materials, due to poor compaction. There was no correlation between forming pressure and composition at a given pellet density. The $KClO_4$ content did not have as much of an impact as did the % TD or Fe type—especially for the Domfer materials.

Break Strength. The mechanical strength of the heat pellets varied depending on the source and size of the Fe in the powder. Figure 11 shows the break strength as a function of

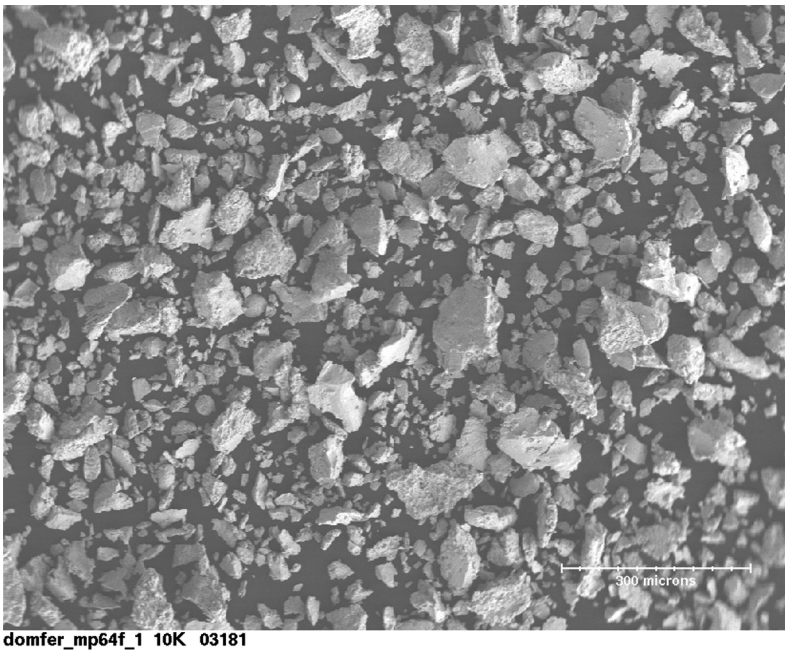

Figure 7. SEM photomicrograph of domfer MP64 Fe powder (300 μm marker).

composition and pellet density. (All compositions used NX-1000 Fe, except for the 80/20 that used EPT Fe.) The break strength increased linearly with pellet density for all compositions, with similar slopes for the various particle sizes of Fe. Larger particle size of Fe (for the same morphology) tended to increase the mechanical strength of the pellet.

Pellets of 84/16 composition made with the Domfer MP31 had a break strength of only 0.25 lb. at 75% TD (not shown in Fig. 11). Similar pellets made with the Domfer MP64 showed an even lower break strength of 0.06 lb. These Fe powders had the largest particle sizes of all the materials examined (Table 2). The low break strengths for these pellets compares to a value of ~7 lb. for the same composition with the NX-1000 Fe.

Pellets with strengths of <1 lb. are too fragile to handle, so the Domfer-based pellets would not be useable. The morphology

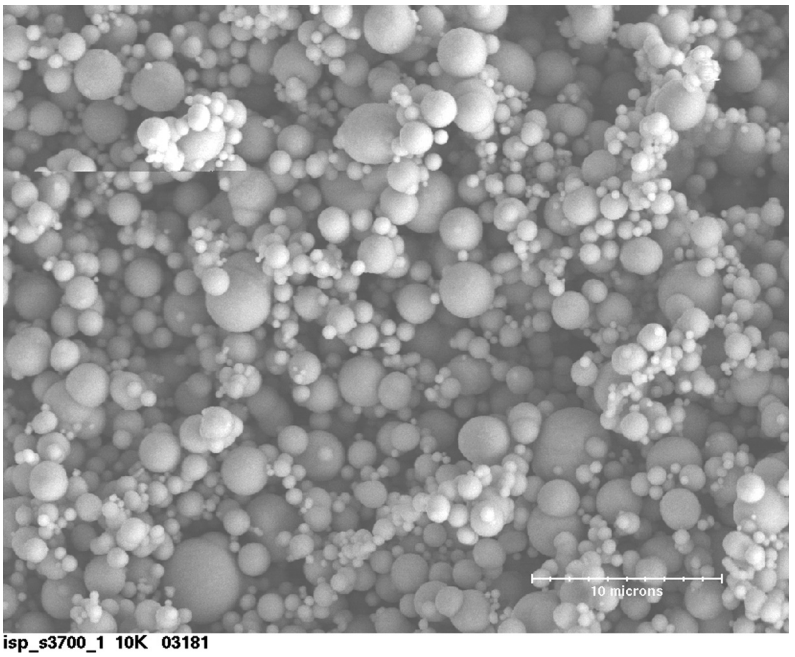

Figure 8. SEM photomicrograph of ISP S-3700 Fe powder (10 μm marker).

of the Domfer Fe and the carbonyl Fe powders makes heat powders with these materials very difficult to compact and the pellets very fragile. These Fe powders lack an interlocking network to reinforce the heat pellet, as is found with the Fe powders used in the UPI, EPT, and PSI heat powders.

Chemical Properties

Fe Purity. The purity of the Fe used in the heat powders will have an impact on the formulation process. When Fe/$KClO_4$ heat powders are blended commercially for SNL, the nominal composition is adjusted to meet a target value specified in SNL's specification drawings. For example, a calorific output of 298 ± 2 cal/g is specified for the 84/16 composition. The actual, final composition of the heat powder will be shifted

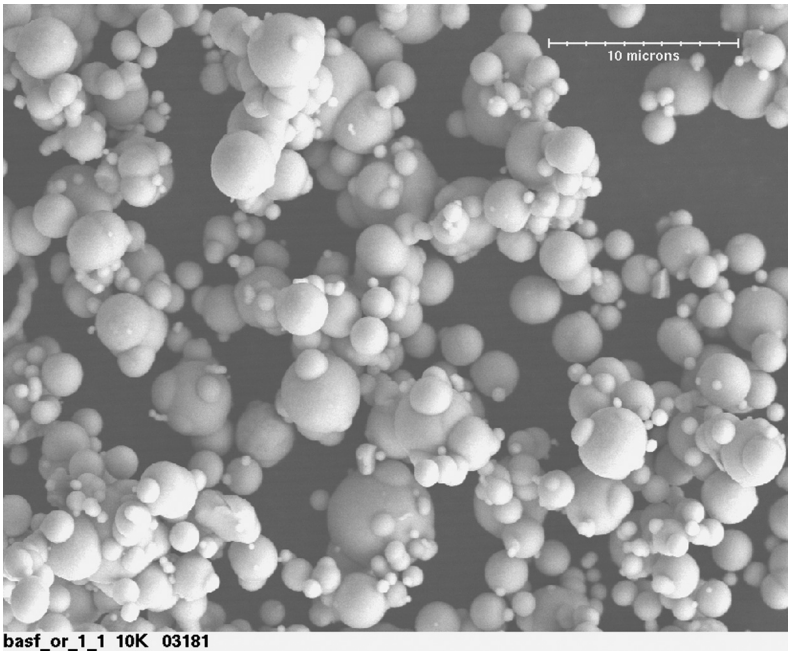

Figure 9. SEM photomicrograph of BASF Fe powder (10 μm marker).

from the nominal value depending on the purity of the Fe. The major impurity in the Fe powder is oxygen, in the form of FeO.

Typical oxygen data for a number of the Fe samples examined in this study are summarized in Table 3. The NX-1000 showed a large range in oxygen levels, from 0.9 to 4.7%. At levels of 1.7% O and greater, lines of FeO became visible in the X-ray diffraction patterns and at 4.7% O, FeO was a minor phase. At the highest level, this corresponds to an FeO content of 21.3%. The carbonyl Fe samples had relatively low oxygen values, with the Domfer Fe oxygen level being comparable to that for NX-1000 Fe. (The effect of oxide impurities on the burn properties of the heat pellets is discussed later in this article.) However, the carbonyl Fe samples had significant levels of carbon and nitrogen of 0.7–0.8%. The Domfer MP64 has the highest carbon level of 3.7%.

Table 1
Physical characteristics of 86/14 heat powders made with various Fe sources

Fe Source	Angle of repose (degrees)	Bulk density (g/cc)	Avg. particle size (μm)*
NX-1000	51.3	1.42	9.8
OMG	N.A.	N.A.	10.8
PSI	45.6	1.63	13.0
ISP S-1000	58.5	2.25	8.8
ISP S-2101	62.3	3.18	4.0
ISP S-3700	66.5	3.03	2.9
BASF 818931	46.6	3.12	4.8
BASF 818941	52.2	3.11	4.9
Domfer MP31	50.0	3.34	38
Domfer MP64	54.0	3.48	64

*As measured by Sedigraph 5000.
N.A. = Not available.

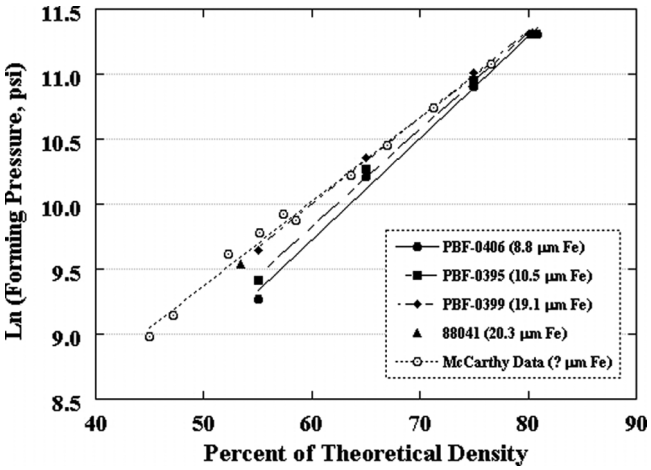

Figure 10. Plot of the logarithm of the forming pressure vs. pellet density for 88/12 Fe/$KClO_4$ heat pellets for various particle sizes of NX-1000 Fe.

Table 2
Forming pressures for some Fe/$KClO_4$ heat pellets

Fe/$KClO_4$ Wt. ratio	Fe source	Avg. Fe particle size (μm)*	% TD	Forming pressure (psi)
88/12	NX-1000	6.3	55	10,590
	〃	6.4		12,220
	〃	9.9		15,480
	〃	13.2		16,300
	〃			
86/14	NX-1000	13.0	55	17,120
	OMG	10.8		11,000
	PSI	13.0		11,900
84/16	NX-1000	8.4	75	46,860
	EPT	10.4		50,520
	Domfer MP31	38		17,110
	Domfer MP64	64		76,270

*As measured by Sedigraph 5000.

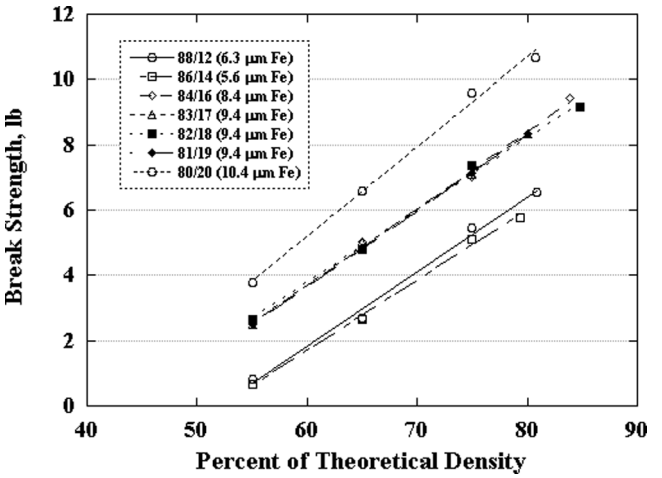

Figure 11. The effect of heat powder composition on the break strength of pellets as a function of density.

Table 3
Oxygen analysis of various Fe sources

Fe source	% O (by inert gas fusion)
NX-1000	0.9–4.7
OMG	1.71
PSI heat powder	1.07
EPT heat powder	1.51
BASF	0.23*
ISP	0.24–0.56*
Domfer	0.73*

*Manufacturer's data.

Combustion Properties

Calorific Output. The measured calorific output of a range of compositions is summarized in Table 4. The 82/18 and 80/20 compositions were made in-house from a commercial 84/16 composition by addition of $KClO_4$. Agreement for replicate samples was very good, with standard deviations of typically $<0.20\%$. Lower than expected calorific outputs were measured for the 82/18 and 80/20 compositions made in house in 1-lb. lots. This reflects the assumption of additivity based on an assumed calorific value for the starting 84/16 blend. Oxide impurities in the Fe will result in lower than expected calorific outputs. Normally, batches of heat powder are made in 100-lb. lots and the composition is adjusted around the nominal value until the desired calorific output is achieved.

The theoretic calorific output of $Fe/KClO_4$ heat powders (based on Eq. (1)) is given by Eq. (2), assuming 100% purity of reactants.

$$\text{Heat Output (cal/g)} = 1,884.73 - 18.8999^{*}(\%\ \text{Fe}) \qquad (2)$$

In the past, there have been differences in the calorific outputs measured and those reported by the manufacturers. Part of this may be due to the measurement techniques used (e.g., adiabatic vs. isoperibolic calorimeter). However, this does not

Table 4
Summary of calorific output measurements performed on Fe/$KClO_4$ heat powders made with NX-1000 Fe

Weight ratio of Fe/$KClO_4$	Lot no.	Average calorific output (cal/g)	Standard deviation*	Specification for output (cal/g)
88/12	PBF-0395	219.9	0.21 (0.10)	219.7–223.7
88/12	PBF-0399	220.4	0.40 (0.18)	219.7–223.7
88/12	PBF-0406	217.9	0.25 (0.11)	219.7–223.7
86/14	PBF-0479	260.8	1.5 (0.49)	257–261
84/16	38934A	295.5	1.27 (0.43)	296–300
82/18	PBF-1642-82-18	329.6	0.45 (0.14)	340 (calc.)
80/20	XHP-SNL 80/20-1	371.0	0.50	372.7 (calc.)
80/20	XHP-SNL 80/20-2	368.8	0.40	372.7 (calc.)

*% Standard deviation is indicated in parentheses.

pose a problem, since the heat requirements for a given thermal-battery design are determined empirically, with a final heat-pellet mass being specified by the design engineer for a specified nominal heat-pellet composition.

Burn Rate. The burn rate of UPI heat pellets of 88/12 composition made with NX-1000 Fe are shown in Fig. 12 as a function of pellet density. (Error bars are shown for one standard deviation about the average.) Data by Evans [4], McCarthy et al. [3], and Reed and Walters [8] are included for comparison and show the same trends that were observed in this work. (Particle size data were not available for these materials.) There was little change in burn rate from densities at the lower limit of ∼45% TD (the lower limit where pellets had structural integrity) to a value of 55–65% TD. Thereafter, the burn rate dropped rapidly as the pellet density was increased. The highest burn rate was exhibited by the material with the smallest particle size of Fe (lot PBF-0406), although the trend in the relative burn rates did not

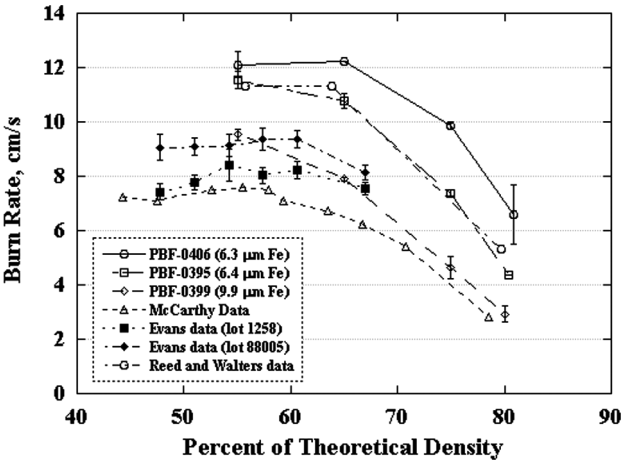

Figure 12. Effect of pellet density and Fe particle size on the burn rate of 88/12 Fe/$KClO_4$ heat pellets made with NX-1000 Fe.

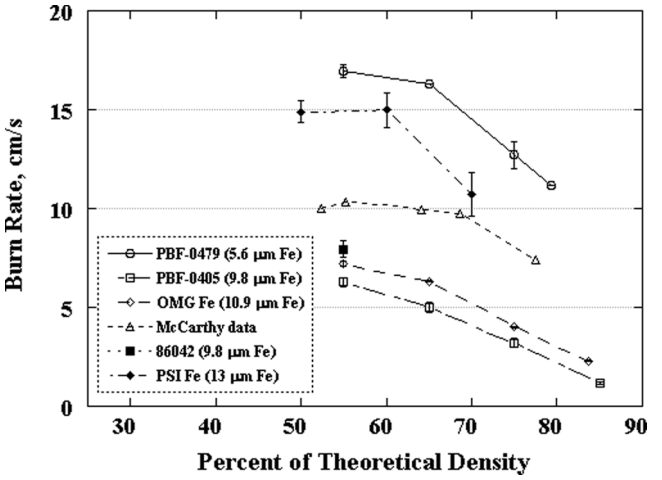

Figure 13. Effect of pellet density and Fe particle size on the burn rate of 86/14 Fe/$KClO_4$ heat pellets.

always follow that of the Fe particle size. There could be differences in the particle size of the $KClO_4$ for the various materials or in Fe purity. The data generated in this work corroborated that reported by Reed et al. [8,9], who used high-speed photography to measure burn rates. The maxima in burn rate tended to shift to higher densities as the particle size of the Fe was reduced. The 88/12 pellets could not be ignited by the laser at densities $>85\%$ TD. It is hypothesized that the increased thermal losses by conduction quenches the burn front under those conditions, so that it does not propagate.

Burn rate data for the UPI 86/14 composition made with NX-1000 Fe are summarized in Fig. 13 along with data for PSI heat powder and a blend made with OMG Fe.[1] In two

[1]It should be noted here that the observed burn rate was affected by the sample weight in tests with this composition. Lower apparent burn rates were observed at intermediate densities (e.g., 60% TD) as the pellet weight was increased. Thus, it is important to use the same mass for all burn rate measurements.

cases, it was possible to attain a density of 85% TD. The OMG and the UPI lot 86042 showed the same trends, with a more rapid drop off in burn rate with increase in pellet density than observed with the UPI lots PBF-0479 and PBF-0405. These latter materials showed a drop-off in burn rate starting between 55 and 65% TD, which is similar to what was observed for the UPI 88/12 heat powders (Fig. 11). Their burn rate behavior was consistent with data reported by McCarthy et al. [3], although the magnitudes were greater. All these powders contained Fe with a similar morphology and particle size.

There was no direct correlation of the Fe particle size and the measured burn rate, although the fastest burning material did have the smallest Fe particle size (5.6 μm). Burn rates for 84/16 heat pellets are reported in Fig. 14 for UPI (NX-1000 Fe) heat pellets and EPT heat pellets as a function of pellet density, along with UPI data by Reed and Walters [8]. Data are also included for pellets made with the BASF ISP S-1000 Fe. At this lower Fe content, it was much easier to attain pellet densities of 85% TD. None of the heat powders made with the carbonyl-Fe sources could be consolidated sufficiently for burn

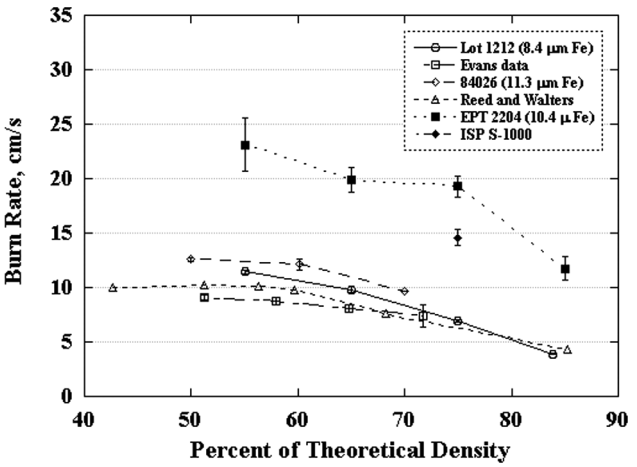

Figure 14. Effect of pellet density and Fe particle size on the burn rate of 84/16 Fe/$KClO_4$ heat pellets.

rate measurements. It was possible to press a blend with ISP S-1000 to 75% TD, however, and those data are included. Reliable ignition of the pellets made with the coarser Domfer MP64 was not possible.

The burn rate peaked at a higher density for the EPT heat pellets (75% TD), relative to that for the UPI heat pellets (55% TD) for a similar average particle size of Fe (10.4 and 11.3 μm, respectively). The EPT heat pellets exhibited twice the burn rate of the UPI pellets, which likely reflects the different source of Fe used. The UPI heat pellets with the smaller average particle size of Fe (8.4 μm) showed a higher burn rate than that with the coarser Fe. The 84/16 heat pellets made with the Domfer MP31 Fe were difficult to ignite and burned very slowly, only 0.24 cm/s at 75% theoretical density (TD), which is more than 40 times slower than pellets made with the NX-1000 Fe.

The burn rates for UPI heat-pellet compositions ranging from 80% Fe to 88% Fe are summarized in Fig. 15 as a function of pellet density. Where possible, data from mixes with comparable Fe particle sizes were used for these comparison. The

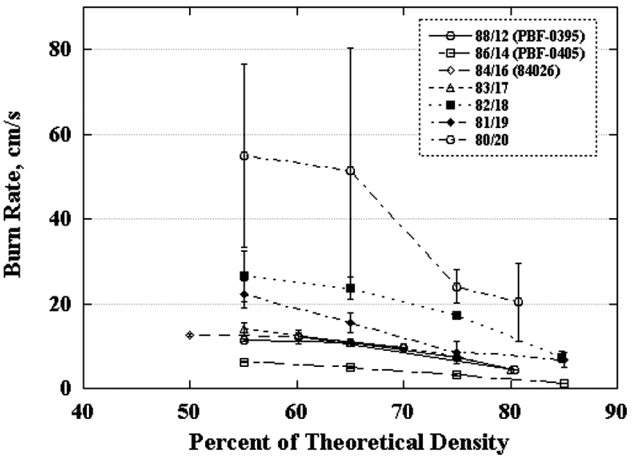

Figure 15. Burn rate of UPI heat pellets as a function of density for various compositions made with NX-1000 Fe.

80/20 heat pellets burned violently, at times breaking apart into small pieces. This composition showed the largest scatter and the highest burn rate. It also had the sharpest drop-off in burn rate with increase in pellet density. The three compositions with the highest $KClO_4$ levels were the only ones that could still be ignited by the laser at 85% TD. The burn rates for these compositions tended to increase with increasing $KClO_4$ content. There was no consistent trend in burn rate with $KClO_4$ content for the full range of compositions, however.

The effects of composition on the burn rate for various pellet densities are summarized in Fig. 16 for UPI heat pellets. (Error bars have been removed for clarity.) Data for samples with comparable particle size were used whenever possible. The rate of increase in burn rate with oxidant content rose dramatically above 18% $KClO_4$ at the lower densities, where burn rates were higher (see Fig. 12).

Since the major impurity in the Fe powder is oxygen, it was desirable to study its impact on burn rate. This was simulated by adding FeO to the heat powder. The effects of added FeO on the burn rate of UPI 84/16 heat pellets at 55% TD are shown in

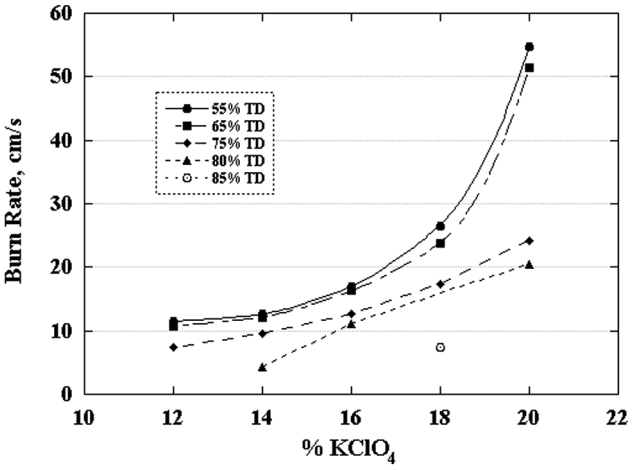

Figure 16. Burn rate of $Fe/KClO_4$ heat pellets as a function of oxidant level for various pellet densities.

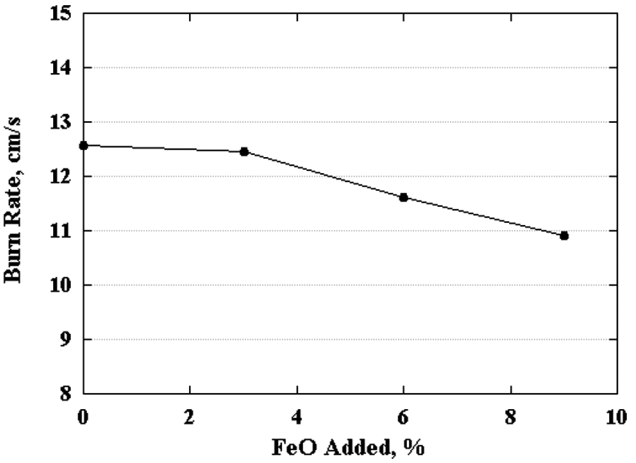

Figure 17. Burn rate of UPI 84/16 Fe/$KClO_4$ heat pellets at 55% TD as a function of added FeO.

Fig. 17. The burn rate was unaffected up to a level of 3% FeO, which corresponds to an oxygen level of 0.791% O in the Fe. At higher levels, the burn rate decreased monotonically with increase in FeO content because of interference with propagation of the burn front due to reduced particle–particle contact throughout the pellet. The highest level of 9% FeO corresponds to 2.37% O in the Fe in the heat powder. Analysis of the Fe used in the heat pellets showed oxygen levels typically between 0.90% and 2.36%, with one value of 4.74% (see Table 3). It should be cautioned, however, that physical addition of FeO may not result in identical effects as bulk oxidation of the Fe in the heat powder.

Peak Temperatures. The temperature profiles during combustion of representative pellet samples of the various UPI heat powder compositions are shown in Fig. 18 for a nominal pellet density of 55% TD. Due to some heat loss where the tip of the pellet protrudes from the sample holder, the peak temperatures are expected to be slightly low. Nevertheless, the trends in the data should still be valid. As expected, the peak temperatures rose

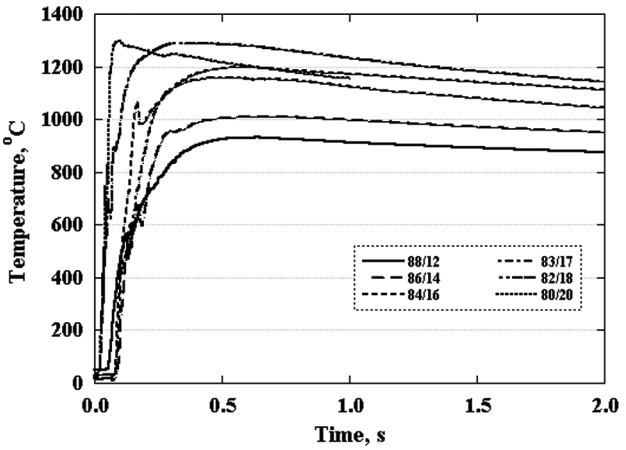

Figure 18. Temperature profiles for various UPI Fe/$KClO_4$ heat pellet compositions during burning (55% TD).

rapidly and the times to peak temperature shifted to lower values as the oxidant level in the heat pellet was increased. The peak temperatures were not greatly influenced by pellet density, except at the highest densities (e.g., 80–85% TD) for the less energetic compositions (88/12 and 86/14).

The effects of Fe type on the peak temperatures are shown in Fig. 19 for an 84/16 composition as a function of pellet density. Pellets made with the UPI and EPT heat powders showed similar peak temperatures, while those for the pellets made with the coarser Domfer MP31 and ISP S-1000 Fe were dramatically lower.

The question arose as to how much of the KCl combustion product is evolved from a heat pellet during the combustion process, since these are used in the confined space of a thermal battery. Three different compositions were examined by leaching away the KCl from the burned pellet and measuring the Cl level in the leach solution. The results of these tests are summarized in Fig. 20. The residual Cl content decreased dramatically as the oxidant level increased due to the higher temperatures and burn rates associated with those compositions. There was <3% Cl left for the 82/18 and 80/20 compositions.

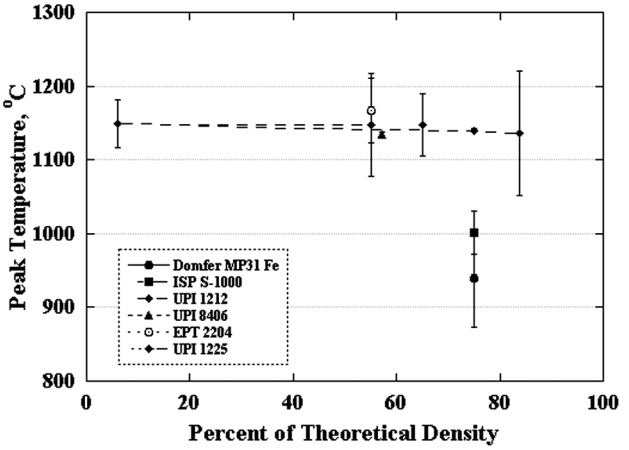

Figure 19. Effect of Fe type on the peak temperatures of 84/16 heat pellets as a function of pellet density.

Ignition Sensitivity. The ignition sensitivity of the various heat powders were determined at the 50th and 90th percentiles. Data in Joules are presented for the 50th percentile as a

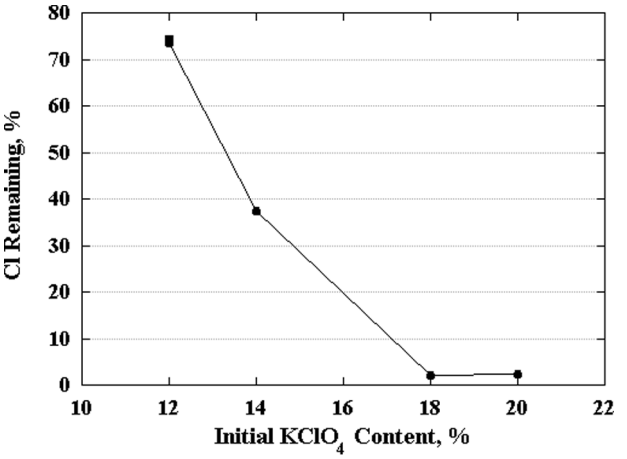

Figure 20. Residual chloride in Fe/$KClO_4$ heat pellets after combustion as a function of initial $KClO_4$ level.

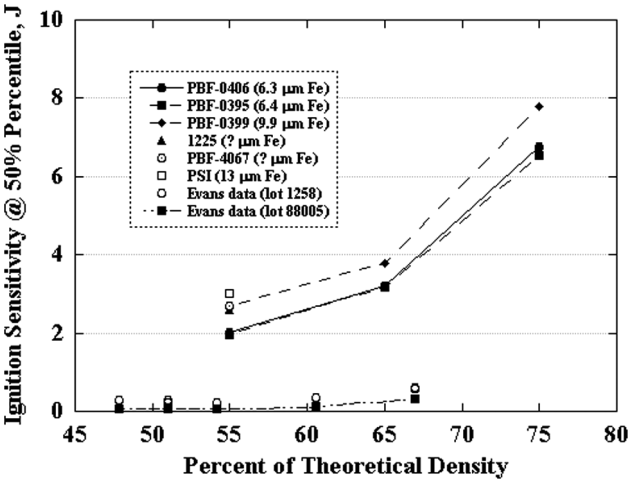

Figure 21. Ignition sensitivity for 50th percentile for 88/12 $Fe/KClO_4$ heat pellets as a function of pellet density.

function of pellet density in Fig. 21 for several lots of UPI 88/12 heat powders and for the EPT heat powder. The energy required for ignition increased in a nonlinear fashion with increase in pellet density. The ignition energies for the pellets with the larger average particle size of Fe (9.9 μm) were slightly greater and offset from the pellets with the smaller average particle size of Fe (6.3–6.4 μm). Similar trends were observed at the 90th percentile.

The ignition sensitivity data reported by Evans [4] were much lower, i.e., ignition took less energy, than observed in this work. This stems from the difference in how the ignition sensitivities were measured in these two studies. Evans used a CD technique in which high voltages (up to 100 V) were applied through electrodes in direct contact with the sample. This results in a different mode of energy transfer compared to the laser technique used in this work.

Ignition-sensitivity data for 86/14 heat pellets are shown in Fig. 22. The ignition energies for the 86/14 heat pellets were almost linear with pellet density, in contrast to the data for the 88/12 composition. The relative differences in the particle

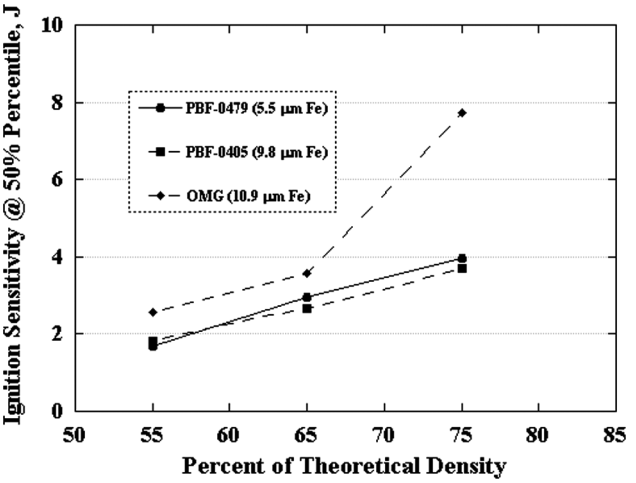

Figure 22. Ignition sensitivity for 50th percentile for 86/14 Fe/$KClO_4$ heat pellets as a function of pellet density.

size of the Fe (5.6 vs. 9.8 μm) did not make a large difference in the ignition sensitivities in this case. The heat powder with the OMG Fe required more energy for ignition relative to those with the NX-1000 Fe and showed more dependence on pellet density.

The ignition sensitivities of 84/16 heat pellets are shown in Fig. 23 and includes data for material with added FeO. The ignition sensitivities of the EPT and UPI heat powders were identical. The heat powder with ISP S-1000 Fe took less energy for ignition and had a somewhat smaller average particle size. The particle sizes of the Fe used in these heat powders ranged from 8.4 to 11.3 μm. At 55% TD, the presence of up to 9% FeO did not impact the ignition sensitivity, as it did the burn rate (Fig. 17). Pellets made with Domfer MP64 could not be ignited by the laser or the hot wire of the bomb calorimeter.

The ignition sensitivities for the various compositions are summarized in Fig. 24 as a function of pellet density. The higher calorific outputs (83/17, 82/18, and 80/20) showed a linear dependency of ignition energy with increase in pellet

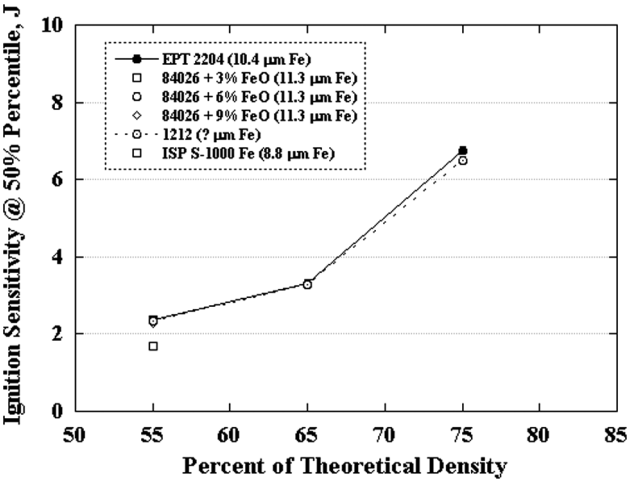

Figure 23. Ignition sensitivity for 50th percentile for 84/16 $Fe/KClO_4$ heat pellets as a function of pellet density.

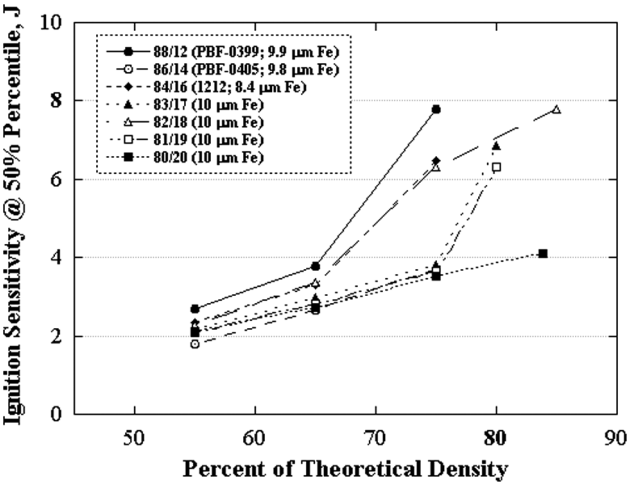

Figure 24. Ignition sensitivity for 50th percentile for $Fe/KClO_4$ heat pellets as a function of composition and pellet density.

density as did the 86/14 composition. Except for this latter material, the energy for ignition showed a decrease with increase in oxidant level. The biggest difference in ignition sensitivity was observed at the higher pellet densities (≥75% TD).

Differential Thermal Analysis (DTA). DTA was examined as a tool for discriminating between various heat powder materials as a function of Fe type and particle size. There were no statistically measured differences among the various materials in the onset temperatures for the phase transition in $KClO_4$ or the exothermic reactions between the Fe and $KClO_4$.

Implications for Use in Thermal Batteries. The mechanical and pyrotechnic properties of the Fe/$KClO_4$ heat pellets impact the performance of thermal batteries that use these materials. In addition to handling and construction issues, weak pellets can lead to crushing and bridging of cells that can result in a thermal runaway in which the battery destroys itself. The use of compositions with higher oxidant contents will result in a higher calorific output per unit weight and volume. This is desirable from a performance perspective in that this would result in a shorter thermal battery stack and a lighter battery. Increased levels of $KClO_4$ will increase the burn rate but would not have a significant effect on the ignition sensitivity. The peak temperatures in the battery stack will also be higher. However, rapid thermal input under these conditions can result in damage to the electrode interfaces in the battery if not moderated. Unfortunately, such heat powders are difficult or prohibitive to ship across the country because of rigorous Department of Transportation (DOT) requirements. In addition, they are more static sensitive in the powder form than the conventional thermal-battery heat powders.

The density of the Fe/$KClO_4$ heat pellets is the dominating factor on performance as it influences both burn rate and ignition sensitivity. High densities (>60% TD) reduce the burn rate and increase the energy for ignition. Higher energy requirements for ignition will increase the likelihood of an ignition failure, which would compromise battery performance—

reliability must be >0.999. Higher burn rates will result in shorter rise times for the battery; i.e., the times for the battery to reach operating temperatures so that power can be drawn. This can be a critical parameter for some applications.

The type of Fe used can have a major impact on the ignition properties as well as the mechanical properties of the $Fe/KClO_4$ heat pellets. The use of spheroidal Fe facilitates the spreading of powder in the die cavity of the press, but results in a weak pellet. Iron with large particle sizes, such as the Domfer materials, result in very low burn rates and high energies for ignition, in addition to poor mechanical pellet integrity. They also did not burn completely. Some pellet compositions with Domfer Fe could not be ignited at all.

By use of the information generated in this study, a battery engineer will be able to apply sound engineering principals to tailor the composition, pellet density, and type of Fe used to meet the thermal requirements for a wide range of thermal-battery applications.

Conclusions

The morphology of the Fe used in $Fe/KClO_4$ heat powders has significant effects on powder properties as well as the mechanical and pyrotechnic properties of pellets pressed from these materials. The flow properties of $Fe/KClO_4$ heat powders are the best when spheroidal carbonyl Fe is used. The acicular Domfer Fe has large particles sizes (up to 64 μm) and results in heat powders with the highest bulk densities of all the mixes examined. Heat powders made with the ISP Fe had the highest angles of repose and therefore the worst flow properties. UPI heat powders with the NX-1000 Fe had the lowest bulk densities and relatively high angles of repose.

The pellet density is the dominating effect on the physical properties and burn characteristics. The logarithm of forming pressure of heat pellets and their break strength show linear responses with increase in pellet density for all compositions. Materials made with the spheroidal carbonyl Fe show the poorest compaction. The weakest pellets are those made with

the Domfer Fe. There is no correlation between forming pressure and the particle size of the Fe.

The density of the heat pellets has a major impact on the burn rate, peaking near 55–65% TD for all compositions and Fe types. At higher densities, the burn rate drops sharply due to quenching of the burn front by the excess Fe present. Burn rates of between 7 and 55 cm/s were measured with peak temperatures of between 900 and 1,300°C. There is a tendency for higher burn rates with a smaller particle size of Fe, although no consistent trend in the burn rate with particle size of Fe is evident. Heat pellets made with Domfer Fe burned an order of magnitude slower than heat pellets with the other types of Fe. As the $KClO_4$ content of the mixture increases, the burn rate also increases, especially at 55 and 65% TD. The most energetic compositions with the NX-1000 Fe tend to burn faster and more violently—especially the 80/20 blend. These latter materials are the only compositions that can be pressed to 85% TD. The addition of FeO contaminant to 84/16 heat powder results in reduced burn rates only at levels $>3\%$.

The 50th percentile ignition energies of the Fe/$KClO_4$ heat pellets range from 1.7 to 7.7 J as determined by a laser technique. These values are much lower than those measured by a CD technique. The ignition energies of heat pellets increase with increasing pellet density and with increase in Fe particle size and tend to decrease with increase in $KClO_4$ content. The morphology of the Fe has a major impact on the ignition sensitivity. Pellets made with the Domfer Fe could not be ignited by the laser or burned in a bomb calorimeter. The presence of up to 9% FeO in the 84/16 heat powder has no effect on the ignition sensitivities.

From a thermal-battery perspective, it is desirable to improve the calorific properties of Fe/$KClO_4$ heat powders by using material with higher $KClO_4$ content, since these materials burn faster and can be ignited more readily at higher densities. However, a variety of shipping restrictions, safety concerns, and possible negative impacts on battery performance caused by the high thermal impulse upon battery activation limit the most energetic composition to an 82/18 blend. Pellet densities in the range of 55–65% provide optimum burn rates and

satisfactory ignition sensitivities. It is desirable to minimize the oxygen level in the Fe to under 1%, so as to not adversely affect the final gravimetric calorific output of the mixture and avoid potentially adverse impacts on performance of the heat powder under certain conditions.

Acknowledgment

Sandia National Laboratories is a multiprogram laboratory operated by Sandia Corp., a Lockheed Martin company, for the United States Department of Energy under contract DE-AC04-94AL85000.

References

[1] 1970. Final Report on the Development of Pelletized Heat Sources for Thermal Batteries Universal Match Co., Unidynamics, Phoenix, AZ. Sandia National Laboratories; Albuquerque, NM. Report SC-CR-70-6137 (final report for Sandia Purchase Order 25-8652).

[2] Guidotti, R. A. 2001. Development History of Fe/$KClO_4$ Heat Powders at Sandia and Related Aging Issues for Thermal Batteries. Sandia National Laboratories; Albuquerque, NM. Report SAND2001-2192.

[3] McCarthy, D. K., W. B. Leslie, and R. W. Dietzel. 1985. Burn Front Velocity as a Function of Pellet Density in Iron/Potassium Perchlorate Heat Powders, Sandia National Laboratories; Albuquerque, NM. Report SAND83-1025.

[4] Evans, T. P. 1984. Ignition Sensitivity Testing: A Preliminary Approach, General Electric Neutron Devices Dept; Pinellas, FL. Thermal Battery Development Report GEPP-TM-814.

[5] Guidotti, R. A., F. W. Reinhardt, and J. Odinek. 2002. Characterization of Fe/$KClO_4$ Heat Powders for Thermal Batteries. Proceedings of the 29th International Pyrotechnics Seminar; Westminster, CO; July 14–19, 2002, 847.

[6] Callaway, J., N. Davies, and M. Stringer. 2002. Pyrotechnic Heater Compositions for Use in Thermal Batteries. Proceedings of the 29th International Pyrotechnics Seminar; Adelaide, Australia, 153–168. In Westminster, CO, July 14–19.

[7] Thomas, E. V. 1993. Evaluating the Ignition Sensitivity of Thermal Battery Heat Pellets. Sandia National Laboratories; Albuquerque, NM. SAND93-0188.

[8] Reed, J. W. and R. R. Walters. 1995. Iron/Potassium Perchlorate Pellet Burn Rate Measurements. Mound Laboratories; Miamisburg, OH. Report MLM-3802.

[9] Reed, J. W., R. A. Walters, R. A. Guidotti, and A. K. Jacobson. 1992. Burn Rate Studies with Iron/Pottassium Perchlorate Heat Pellets; Proceedings of the 35th International Power Sources Symposium, Cherry Hill, NJ, June 22–25, 1992, 211.